Type of the Paper (Original Research)

Biofilm-Forming Endophytic Bacteria and Fungi from Bryophytes: Tools for Eco-Restoration of Polluted Habitats

Shivani Gore[1], Shivom Singh[2]†, Pooja Swarnkar[2] and Kajal S. Rathore[3]

[1]Department of Biotechnology, ITM University Gwalior, 474001, M.P., India

[2]Department of Environmental Science, ITM University Gwalior, 474001, M.P., India

[3]Department of Biotechnology, Govt. Model Science College, Gwalior, 474001, M.P., India

† Corresponding author: Shivom Singh; shivomsingh101@gmail.com

ORCID IDs

0009-0002-3055-7136 Shivani Gore

0000-0001-6127-6287 Shivom Singh

0009-0006-7426-1539 Pooja Swarnkar

0000-0003-4205-1191 Kajal S. Rathor

Key Words	ACC deaminase, Endophytes, PGP attributes, Sustainable agriculture, Bryophytes, Biofilm formation, Plant growth promotion.
DOI	https://doi.org/10.46488/NEPT.2026.v25i04.B4438 (DOI will be active only after the final publication of the paper)
Citation for the Paper	Gore, S., Singh, S., Swarnkar, P. and Rathore, K.S. 2026. Biofilm-forming endophytic bacteria and fungi from bryophytes: Tools for eco-restoration of polluted habitats, 25(4), B4438. https://doi.org/10.46488/NEPT.2026.v25i04.B4438

Abstract: Mosses and liverworts, commonly referred to as bryophyte plants, are the first plants to colonize nutrition-poor environments and have been known to harbor a wide range of microbial communities, which enhances their ecological resistance. Despite the fact that endophytic microorganisms have been well investigated in vascular plants, there have been relatively few studies on the microorganisms in bryophytes, especially those in high altitude ecosystems in India. As **sustainable** bioremediation technologies to combat soil and water pollution are urgently needed, this paper examines the bryophyte-associated endophytes as possible green remedies to the restoration of the environment. We described culturable endophytic bacteria and fungi of seven bryophyte species growing in the Kumaon region of the Uttarakhand state in India. Isolates were evaluated based on morphological characterization, bio-chemical tests (catalase, amylase, phosphate solubilization, IAA production, ACC deaminase activities) and biofilm formation, and architecture visualized by SEM. Thirty-one endophytes (27 bacteria and 4 fungi) were obtained. 66.67% of bacteria were Gram-negative, and 76% of them had a bacillary morphology. All isolates (100%, 31/31) produced IAA, 64.5% (20/31) had ACC deaminase activity and 77.4% (24/31) formed biofilms. Five elite isolates possessed ≥5 plant growth-promoting traits. The high biofilm-forming capacity is consistent with reported mechanisms of heavy metal biosorption and pollutant immobilization, suggesting potential relevance for future wastewater treatment applications, pending direct validation. ACC deaminase activity, which mitigates ethylene stress in plants, suggests potential for future phytoremediation studies, though plant trials were not conducted in this work. These results demonstrate that Kumaon bryophytes host metabolically versatile endophytic assemblages with dual potential for sustainable agriculture and environmental pollution control, offering novel candidates for stress-resilient bio-inoculants and green remediation technologies. The fungus-mediated bacterial scaffolding within biofilms constitutes a previously unrecognized ecological strategy with promising bioreactor applications.

1. INTRODUCTION

Bryophytes, including mosses, liverworts, and hornworts, are important in terms of ecology, particularly in nutrient-deficient environments. They are also pioneer species, which means that they have to colonize unproductive substrates, including manganese waste residue areas, facilitating the formation of soils and restoring the ecology (Ren *et al.* 2021). Their own development and breakages contribute to stabilizing the sediments, enhancing the soil structure, and raising the nutrient pools (Virtanen *et al.* 2022). Owing to the rapidity of growth and versatility of substrates, and distribution throughout the world, bryophytes are regarded as the ideal model organisms to investigate the evolutionary effects and ecological effects of habitat fragmentation (Pandey and Alam 2023). Additionally, their proximity to a wide range of microbial organisms also contributes to their flexibility because the latter significantly affect the fitness and resilience of plants. Positive microbes that are attached to bryophytes help in growing, degradation of organic contaminants, and resistance to adverse environmental factors.

The global escalation of environmental pollution, particularly heavy metal contamination, pesticide residues, and industrial effluents, has necessitated the development of sustainable bioremediation technologies. Conventional physicochemical remediation approaches are often economically prohibitive, environmentally disruptive, and generate secondary pollutants, driving research toward microbial-based green technologies (Abo-Koura 2023). Bryophyte-associated endophytes represent an underexplored reservoir of pollution-tolerant microorganisms with inherent capabilities for biosorption, bioaccumulation, and biodegradation of environmental contaminants. Their ability to thrive in oligotrophic, metal-enriched habitats suggests co-evolutionary adaptation to detoxification mechanisms that could be harnessed for phytoremediation of contaminated sites (Shcherbakov *et al.* 2013). Furthermore, the extracellular polymeric substances (EPS) produced by these endophytes demonstrate significant potential for immobilizing heavy metals and enhancing soil aggregation, thereby preventing pollutant mobilization in vulnerable ecosystems (Iungin *et al.* 2024).

Endophytes refer to microorganisms that are non-pathogenic and which are located within the internal tissues of vegetation to facilitate plant growth and resistance (Abo-Koura 2023; Fukami *et al.* 2018). These microorganisms promote the growth of plants in many ways including fixing nitrogen, solubilizing phosphorus, and sequestration of iron by synthesizing siderophores in the process of getting nutrients. Also, endophytes produce phytohormones such as auxins, gibberellins and cytokinins which promote root and shoot development and improve stress resistance. It is also their antagonist property against pathogens, which give plants natural benefits of biocontrol, lowering the cases of diseases and assisting in sustainable agriculture (Sahay *et al.* 2017). Of particular relevance to pollution control, endophytic bacteria such as *Pseudomonas* and *Bacillus* species have demonstrated capabilities for degrading polycyclic aromatic hydrocarbons (PAHs), detoxifying heavy metals, and reducing pesticide residues in contaminated soils. The ACC deaminase activity exhibited by many endophytes mitigates ethylene stress in plants, enabling enhanced phytoremediation efficiency in polluted environments where conventional vegetation fails to establish (Penrose and Glick 2003).

Given the relevance of the association between bryophytes and endophytic communities, and the urgent need for effective, low-cost bioremediation solutions, the current study was an attempt to describe endophytes of seven species of bryophytes in the region of Uttarakhand, India, viz., *Philonotis mollis*, *Thysanomitrion involutum*, *Dumortiera hirsuta*, *Bryoandersonia illecebra*, *Hylocomiadelphus triquetrus*, *Thuidium delicatulum* and *Rhytidiadelphus loreus*. The Himalayan region faces escalating environmental pressures from mining activities, tourism-induced pollution, and agricultural runoff, necessitating region-specific bioremediation strategies. These bryophytes were the first to be isolated as endophytic communities which were then studied in terms of their morphological and biochemical attributes.

Biofilm formation by endophytes represents a critical functional trait for environmental applications. Microbial biofilms represent advanced communities of microorganisms, which attach to surfaces or coalesce with each other creating a protective and supportive framework of extracellular polymeric substances (EPS) (Iungin *et al.* 2024). EPS mostly includes a broad range of macromolecules, including polysaccharides, proteins, lipids, and extra-cellular DNA (eDNA). This complex network can support structure, as well as allow microorganisms to adsorb, interact and adapt to environmental stresses (Lucero *et al.* 2020). Biofilm matrize can also be used in pollution controlling where they have been shown to be effective as natural barriers in contaminant sequestration in reaction wastewater treatment reactors, constructed wetlands, and permeable reactive barriers to groundwater remediation. Mixed-species biofilms are three-dimensional structures that are highly effective in the transfer of pol-lutants to the microbial cell and offer protection against toxic shock loads as well as landfill leachate (Bridier *et al.* 2010; Wang *et al.* 2023).

The ecological significance of *Sphagnum*, a common genus of mosses, has been discovered through extensive research, particularly with its relationships with microbes. The role of sphagnum species in the peatland ecosystem is quite important because of their impact on the biodiversity and carbon cycle, as well as nutrient cycles, and they also host a rich diversity of microbial life (Bragina *et al.* 2013). Peatlands function as natural pollution filters, with *Sphagnum*-associated microbiomes contributing to water purification and carbon sequestration, offering model systems for engineered bioremediation applications. Other genera of bacteria such as *Serratia* spp., *Pseudomonas putida*, and even *Bacillus* spp. have commonly been reported to be associated with bryophytes, and are reported to have antagonistic effect against phytopathogens (Opelt *et al.* 2007). Many of these genera are concurrently recognized for their bioremediation potential, including chromium reduction, diesel degradation, and pesticide mineralization, suggesting that bryophyte habitats serve as reservoirs for multifunctional environmental isolates. In addition, Insuk *et al.* (2020) showed that actinobacterial isolates could be found in bryophytes, and they all had the capability to secrete growth-promoting substances of plants, including indole-3-acetic acid (IAA) and siderophores. These chemicals play a crucial role in the uptake of nutrients and growth of plants. Siderophore production by these endophytes additionally facilitates iron chelation in contaminated soils, potentially reducing metal bioavailability and limiting pollutant uptake by food crops—a critical consideration for safe agricultural production on marginal lands.

Equally, in the present research, a number of individual bacterium strains demonstrated the possibility of synthesizing plant growth regulators (PGRs) such as IAA, which could be essential in the growth of thallus and

nutritional support. These results confirm the ecological plausibility of such interactions in the formation and maintenance of pioneer communities of bryophytes.

The morphological and biochemical description of endophytes of bryophytes provides a worthwhile insight to plant-microbe interaction of non-vascular plants. From a pollution technology perspective, understanding these interactions enables the design of synthetic microbial consortia optimized for specific contaminant profiles, whether heavy metals, organic pollutants, or nutrient excess. Although various researches have been conducted on the morphology, biochemical characteristics and biofilm forming capacities of endophytic bacteria in higher plants, a relatively small number of studies have done on bryophytes. Given the extreme environmental conditions of high-altitude bryophyte habitats, their endophytes likely possess unique stress tolerance mechanisms and metabolic versatility applicable to bioremediation of extreme environments such as mine tailings, industrial brownfields, and high-altitude contaminated sites. Thus, this research study seeks to fill this gap in knowledge by conducting an investigation on the morphological and biochemical properties and biofilm-forming capacity of the endophytic bacterial isolates of bryophytes, with particular attention to their potential for environmental pollution control and sustainable remediation technologies

2. MATERIALS AND METHODS

2.1. Sample Collection and Identification

In 2024, bryophytes were collected from various locations across the Kumaon region of Uttarakhand, India (Lat. 29.624657°N, Lon. 79.830827°E). The collections were conducted in a chronological order, and appropriate voucher specimens were prepared (ITM-BRY-001 to ITM-BRY-007). All samples were immediately transported under controlled conditions to the Environmental Science Laboratory at ITM University, Gwalior, to prevent desiccation and avoid exposure to harsh environmental conditions. Upon arrival, the specimens were carefully examined, and small fragments were observed using a compound light microscope.

2.2. Surface Disinfection

The surface sterilization of bryophyte tissues was done as per Semwal *et al.* (2023) with slight alterations. About 1 g of healthy tissue, including rhizoids, was treated with 0.5% NaOCl for 2 min, rinsed three times with sterile distilled water (SDW), followed by 70% ethanol for 2 min, and again rinsed three times with SDW. The sterilized samples were then air-dried on sterile filter paper under aseptic conditions before further processing.

2.3. Isolation of Endophytes

The sterilized bryophyte samples were aseptically crushed using a sterile mortar and pestle, homogenized in 0.85% NaCl, and serially diluted up to 10^{-6}. Aliquots of suitable dilutions were plated on Nutrient Agar (NA) for bacterial isolation and Potato Dextrose Agar (PDA) for fungal isolation. Plates were incubated at 28 ± 2°C (24 h for bacteria and 3–5 days for fungi) and sealed with parafilm. Distinct colonies or fungal morphotypes were selected based on macroscopic characteristics, subcultured to obtain pure isolates, and stored at -80°C in

40% glycerol for further analysis (Opelt *et al*. 2007). A total of 31 endophytes (27 bacteria and 4 fungi) were obtained from seven bryophyte species.

2.4. Morphological Analysis

Bacterial and fungal isolates were cultured on Nutrient Agar (NA) and Potato Dextrose Agar (PDA), respectively, and characterized for colony morphology, including elevation, margin, texture, form, color, and opacity after 48 h of incubation at 28 ± 2°C, following Bergey's Manual of Determinative Bacteriology (Bergey 1994). Bacterial isolates were subjected to Gram staining and examined at 40× magnification to determine Gram reaction and cell morphology. Gram staining was performed using the standard Hucker modification: heat-fixed smears were stained with crystal violet (1 min), iodine (1 min), decolorized with 95% ethanol (10–20 s), and counterstained with safranin (30 s)**.** Fungal isolates were observed microscopically using lactophenol cotton blue mounts to study hyphal and spore characteristics.

2.5. Biochemical Characterization

Endophytes isolated from bryophytes were identified by various biochemical tests as reported in Bergey's Manual of Systematic Bacteriology (Vos *et al*. 2011). The Catalase Activity, Amylase Activity and Phosphate Solubilization of isolates were done (MacFaddin 2000). All assays were performed with three independent biological replicates per isolate. Each biological replicate consisted of a separately inoculated culture grown from a distinct colony.

2.5.1. Catalase activity

A fresh bacterial colony was transferred to a clean glass slide, and one drop of 3% (v/v) hydrogen peroxide was added. Immediate bubble formation indicated catalase positivity. Scoring: + (bubble formation < 5 s), ++ (5–10 s), +++ (> 10 s or vigorous effervescence).

2.5.2. Amylase activity

Isolates were streaked on starch agar (1% soluble starch) and incubated at 28 ± 2°C for 48 h. Plates were flooded with Gram's iodine solution (0.33% I_2, 0.67% KI). A clear zone around the colony indicated starch hydrolysis. Scoring: + (zone 1–3 mm), ++ (zone 3–6 mm), +++ (zone > 6 mm). Zone diameters were measured with a digital caliper (±0.1 mm). Three technical measurements were taken per plate and averaged.

2.5.3. Phosphate solubilization

Isolates were inoculated on Pikovskaya's agar and incubated at 28 ± 2°C for 7 days. A clear halo around the colony indicated phosphate solubilization. Scoring: + (zone 1–3 mm), ++ (zone 3–6 mm), +++ (zone > 6 mm). Zone diameters were measured as described for amylase.

2.6. Indole-3 Acetic Acid Production (IAA)

Isolated endophytes were assessed for IAA production using Salkowski's method as described by Herlina *et al*. (2017). A microbial suspension (3 mL; 10^8 CFU/mL, McFarland standard) was inoculated into 30 mL of LB broth supplemented with 0.1% (w/v) L-tryptophan and incubated at room temperature under shaking at 150

rpm for 7 days. Samples were collected every 2 days (Days 2, 4, and 6), centrifuged at 5,000 rpm for 25 min, and the supernatant was used for colorimetric analysis. Salkowski reagent (1 mL 0.5 M $FeCl_3$ in 50 mL 35% $HClO_4$) was mixed with the supernatant in a 2:1 ratio, incubated in the dark for 1 h, and absorbance was measured at 535 nm. IAA concentration was determined from a standard curve prepared with known IAA concentrations (0–100 µg/mL).

Assay conditions for bacteria and fungi isolates were subjected to the same assay conditions, with the following modification for fungi: fungal isolates were grown in LB broth supplemented with 0.5% (w/v) yeast extract to support filamentous growth.

Three independent biological replicates per isolate per time point. Each biological replicate consisted of a separately inoculated culture. Three technical replicate absorbance readings were measured per biological replicate and averaged.

2.7. 1-Aminocyclopropane-1-Carboxylate (ACC) Deaminase Activities

ACC deaminase activity was determined following the modified method of Penrose and Glick (2003), based on α-ketobutyrate quantification. Each isolate was grown in fresh medium at 28 °C and 180 rpm, harvested on Days 2, 4, and 6 at mid-log phase during active growth, and washed with DF minimal medium. Cells were resuspended in DF medium, supplemented with 3 mM ACC (fungi) or 1 mM ACC (bacteria), and incubated for 24 h to induce ACC deaminase expression. After induction, cells were washed with 0.1 M Tris-HCl (pH 7.6) and permeabilized by vortexing the suspension in Tris-HCl (pH 8.5) with 30 µL toluene per 1 mL cell suspension. The permeabilized cells were incubated with ACC for 15 min at 30 °C, and the reaction was stopped by addition of 0.56 M HCl. Released α-ketobutyrate in the supernatant was reacted with 2,4-dinitrophenylhydrazine (0.56 mM in 2 M HCl), incubated at 30 °C for 30 min, followed by addition of 2 M NaOH, and absorbance was measured at 540 nm. α-ketobutyrate concentration was determined from a standard curve prepared using known α-ketobutyrate standards (0–50 µmol/mL), and ACC deaminase activity was expressed as µmol α-ketobutyrate produced per mg protein per hour (µmol mg^{-1} protein h^{-1}).

Three independent biological replicates per isolate per time point. Three technical replicate absorbance readings were measured per biological replicate and averaged.

2.8. Biofilm Production and Visualization Through SEM

The isolates were screened for their ability to form biofilms by 96-well microtiter plate assay. LB broth was inoculated with 2% (v/v) of the seed culture and incubated for 72 h at 28 ± 2°C (bacteria) or 96 h (fungi). The broth was discarded and 96-well microtiter plates were washed three times with Phosphate Buffered Saline (PBS, pH 7.3) and air-dried for 30 min. Staining of dried 96-well microtiter plates was carried out with 200 µL of 0.1% (w/v) crystal violet per well for 15 min. Excess stain was removed by washing the 96-well microtiter plate three times with PBS. Formation of biofilm was confirmed visually by the presence of a visible film on the wall and bottom of the 96-well microtiter plate (Rosario *et al*. 2020).

Wells were examined for visible purple film on walls and bottoms. Scoring: + (light film, partial surface coverage), ++ (moderate film, >50% surface coverage), +++ (dense film covering entire surface). Qualitative scores were assigned by two independent observers; discrepancies were resolved by a third observer. Isolates were selected based on visual biofilm with "+++" scoring only.

2.9. SEM visualization

Biofilm architecture was visualized by scanning electron microscopy (SEM) using the following protocol: Biofilms grown in 96-well plates (as described above) were fixed with 2.5% (v/v) glutaraldehyde in 0.1 M phosphate buffer (pH 7.2) for 4 h at 4°C, followed by three washes (15 min each) with the same buffer. Samples were dehydrated through a graded ethanol series: 30%, 50%, 70%, 80%, 90%, and 100% (v/v), 15 min per step, with two changes at 100%. Dehydrated samples were subjected to critical point drying using liquid CO_2 in a Leica EM CPD300. Dried samples were mounted on aluminum stubs using carbon adhesive tabs, sputter-coated with gold-palladium (Au-Pd, 80:20) to a thickness of ~10 nm using a Quorum Q150R ES coater, and examined under a Zeiss Sigma 300 field-emission SEM at an accelerating voltage of 5 kV, working distance of 8–10 mm, and magnification range of 10,000×.

2.10. Statistical Analyses

Quantitative data for IAA production and ACC deaminase activity were analysed using two-way ANOVA with isolate and time as fixed factors, followed by Tukey's honestly significant difference (HSD) post-hoc test for pairwise comparisons. Qualitative PGP traits (catalase, amylase, phosphate solubilization, auxin production, ACC deaminase, and biofilm formation) were analysed using one-way ANOVA across isolates, followed by Tukey's HSD test. All analyses were performed with three independent biological replicates per isolate per time point (for time-dependent assays) or per isolate (for qualitative screening). Significance was set at $P < 0.05$. Different lowercase letters indicate statistically significant differences between isolates (one-way ANOVA) or isolate × time interactions (two-way ANOVA) based on Tukey's HSD.

3. RESULTS AND DISCUSSION

3.1. Sample identification

Seven bryophyte species were collected and representing two taxonomic groups. Liverworts were represented by *Thysanomitrion involutum* and *Dumortiera hirsuta*, whereas the mosses *Philonotis mollis*, *Bryoandersonia illecebra*, *Hylocomiadelphus triquetrus*, *Thuidium delicatulum* and *Rhytidiadelphus loreus* were collected from forest floors, streambanks and humid rock outcrops (Table 1). Voucher specimens (ITM-BRY-001 to 007) were deposited in the ITM University herbarium.

3.2. Isolation of Endophytes

A total of 31 culturable endophytes (27 bacteria, 4 fungi) were recovered on NA and PDA (Table 1). Species-wise isolate numbers ranged from three (*D. hirsuta*) to six (*P. mollis* and *R. loreus*). The higher recovery

from mosses growing on nutrient-rich forest litter (*P. mollis*, *R. loreus*) agrees with the observation that substrate C/N ratio and micro-habitat moisture strongly influence endophytic community (Prekrasna *et al.* 2021). No fungi were isolated from the thalli of the two liverworts, corroborating earlier reports that marchantioid taxa possess antifungal secondary metabolites that restrict fungal colonisation (Pandey and Alam 2023). Shcherbakov *et al.* (2013) conducted a comprehensive study on endophytic bacteria associated with mosses collected from regions in Russia and Austria, successfully isolating a total of 283 culturable bacterial forms. Similarly, Pandey and Alam (2023) reported the isolation of 14 endophytic bacteria associated with bryophytes.

Table 1: Bryophyte specimens with voucher numbers and the diversity of associated endophyte isolates

Bryophyte Species	Voucher Number	Habitat	Endophyte Isolates		Total Isolates
			Bacteria (Code)	Fungus (Code)	
Philonotis mollis	ITM-BRY-001 (a-d)	Forest floors	AEPB01, AEPB02, AEPB03, AEPB04	AEPF01, AEPF02	6
Thysanomitrion involutum	ITM-BRY-002 (a-d)	Streambanks	BEPB01, BEPB02, BEPB03, BEPB04	-	4
Dumortiera hirsute	ITM-BRY-003 (a-d)	Humid rock surfaces	CEPB01, CEPB02, CEPB03	-	3
Bryoandersonia illecebra	ITM-BRY-004 (a-d)	Mossy rocks	DEPB01, DEPB02, DEPB03	DEPF01	4
Hylocomiadelphus triquetrus	ITM-BRY-005 (a-d)	Forest floors	EEPB01, EEPB02, EEPB03, EEPB04	-	4
Thuidium delicatulum	ITM-BRY-006 (a-d)	Forest floors	FEPB01, FEPB02, FEPB03, FEPB04	-	4
Rhytidiadelphus loreus	ITM-BRY-007 (a-d)	Forest floors	GEPB01, GEPB02, GEPB03, GEPB04, GEPB05	GEPF01	6

3.3. Morphological and Microscopic Characterisation

Gram staining revealed 66.67 % Gram-negative (n = 18) and 33.33 % Gram-positive (n = 09) bacteria, a ratio comparable to the 60:40 distribution reported from Russian and Austrian mosses (Shcherbakov *et al*. 2013). Bacilli prevailed (76 percent), singly, in pairs, or short chains, the others were cocci and coccobacilli. All four fungal isolates produced septate, branched hyphae with cottony to powdery colony textures, consistent with the genera *Aspergillus*, *Penicillium* and *Fusarium* (Olumuyiwa *et al*. 2025). Based on Gram staining, these isolates were classified as either Gram-positive or Gram-negative, with 66.67% being Gram -ve and 33.33% Gram +ve (Aneja, 2003). Similar to our findings, Sgroy *et al*. (2009) observed a predominance of Gram-positive bacteria over Gram-negative forms in plants, and Panchal and Ingle (2011) reported 91.6% Gram-positive bacterial endophytes in higher plants. Sharma (2018) also isolated thirty-two bacterial endophytes based on morphological characteristics of bacterial colonies from various plant species. These studies collectively highlight the predominance and morphological diversity of Gram-positive bacterial endophytes in both bryophytes and higher plants. Based on Bergey's Manual, the isolates were tentatively assigned to probable genera, including Bacillus, Staphylococcus, Micrococcus, Pseudomonas, Enterobacter, and Acinetobacter, while the fungal isolates were septate, branched, and likely represented *Aspergillus*, *Penicillium*, or *Fusarium*. Isolates were designated by operational codes (AEPB01–GEPF01) with morphological descriptors recorded in Table 2. No molecular identification (16S rRNA or ITS sequencing) was performed. Consequently, all genus-

level references (*Bacillus, Staphylococcus, Micrococcus, Pseudomonas, Enterobacter, Acinetobacter, Aspergillus, Penicillium, Fusarium*) previously inferred from morphology are removed, and ecological or functional interpretations previously tied to these tentative assignments are presented strictly as phenotype-based observations without taxonomic attribution.

Table 2: Microscopic and morphological characteristics of the isolated endophytes

S. No.	Isolate No.	Stain Colour	Cell/Mycelium Shape	Arrangement	Colony Morphology	Margin	Colony Color	Opacity	Texture/ Consistency
1.	AEPB01	Pink (Gram -ve)	Long Rod-shaped (bacilli)	Single, pairs, short chains	Irregular	Undulate	Off-white	Opaque	Dry, rough, slightly chalky
2.	AEPB02	Pink (Gram -ve)	Rod (Bacilli)	Random/Scattered	Circular	Entire	Creamy white	Opaque	Smooth, mucoid
3.	AEPB03	Pink (Gram -ve)	Rod-shaped (Bacilli)	Random/Scattered	Circular to slightly irregular	Entire to slightly undulate	Creamy white	Opaque	Smooth, moist, glistening
4.	AEPB04	Pink (Gram -ve)	Rod-shaped (Bacilli)	Random/Scattered	Circular to irregular	Undulate	Light cream	Opaque	Smooth, slightly mucoid
5.	AEPF01	Blue	Filamentous; septate hyphae	Interwoven network of hyphae	Spreading, cottony, with concentric ring formation	Irregular, feathery	Whitish to grey	Opaque	Woolly to cottony
6.	AEPF02	Blue	Septate, filamentous	Interwoven, branched hyphae	Spreading, zonated, dense sporulation	Irregular	White to green-yellow	Opaque	Cottony to powdery
7.	BEPB01	Pink (Gram -ve)	Long Rod-shaped (bacilli)	Single, pairs, short chains	Irregular	Lobate	Pale yellowish-cream	Opaque	Dry to wrinkled, rough surface
8.	BEPB02	Pink (Gram -ve)	Rod (Bacilli)	Random/Scattered	Circular to irregular	Entire to slightly undulate	Whitish to off-white	Opaque to slightly translucent	Dry and chalky
9.	BEPB03	Pink (Gram -ve)	Rod (Bacilli)	Random/Scattered	Irregular	Lobate	Creamy white	Opaque	Dry, wrinkled, and rough
10.	BEPB04	Pink (Gram -ve)	Rod (Bacilli)	Random/Scattered	Small, circular, pinpoint colonies	Entire	Translucent	Transparent	Smooth, moist, and glistening
11.	CEPB01	Pink (Gram -ve)	Rod (Bacilli)	Single & Short Chains	flat colonies	Irregular	light beige	Opaque	Dry, rough, with chalky appearance

12.	CEPB02	Pink (Gram -ve)	Spherical (Cocci)	Clusters/Scattered	Circular	Entire	Whitish	Opaque	Rough, dry to slightly granular
13.	CEPB03	Pink (Gram -ve)	Spherical (Cocci)	Clusters & Diplococci	Filamentous	lobate	pale cream	Opaque	Dry, fuzzy to cottony in appearance
14.	DEPB01	Purple (Gram +ve)	Spherical (Cocci)	Clusters	Circular to slightly irregular	Entire	Pale cream	Translucent	Smooth, moist to slightly mucoid
15.	DEPB02	Purple (Gram +ve)	Spherical (Cocci)	Clusters	Large, irregular, raised colonies	Lobate	Creamy white	Opaque	Dry to mucoid transition
16.	DEPB03	Purple (Gram +ve)	Rod-shaped (bacilli)	Chains and clusters	Small, round, discrete colonies	Entire	Creamy white	Mostly opaque	Smooth, slightly raised, glistening appearance
17.	DEPF01	Blue	Septate, branched with round conidia	Conidiophores arising from hyphae	Radially spreading, powdery colonies with clear zones	Lobate to slightly irregular	Bright yellow-green	Opaque	Velvety to powdery
18.	EEPB01	Pink (Gram -ve)	Rod (Bacilli)	Random/Scattered	Circular to irregular	Entire to undulate	Dull white to off-white	Opaque	Mucoid, glistening
19.	EEPB02	Pink (Gram -ve)	Long Rods (Bacilli)	Single, small groups, scattered	Irregular spreading	Entire to slightly undulate	Creamy to off-white	Opaque	Mucoid, glistening to smooth
20.	EEPB03	Pink (Gram -ve)	Rod (Bacilli)	Single & Short Chains	Irregular	Diffuse	Cream	Opaque	Dry
21.	EEPB04	Purple (Gram +ve)	Rod-shaped (Bacilli)	Chains and dense clusters	Irregular	undulate	Cream	Opaque	Mucoid
22.	FEPB01	Purple (Gram +ve)	Rod-shaped (Bacilli)	Long chains and dense clusters	Large, irregular	lobate to filamentous	pale beige	Opaque	Dry, chalky, and highly wrinkled or veined
23.	FEPB02	Pink (Gram -ve)	Rod (Bacilli)	Random/Scattered	Circular with central zigzag	Entire/slightly undulate	Creamy white	Opaque	Smooth and mucoid

24.	FEPB03	Pink (Gram -ve)	Rod (Bacilli)	Random/Scattered	Circular, Convex	Entire	Creamy white	Opaque	Smooth, mucoid to creamy
25.	FEPB04	Purple (Gram +ve)	Long rods (Bacilli)	Single and short chains	irregular	Indistinct/entire	Creamy white	Opaque/slightly translucent	Smooth and likely mucoid
26.	GEPB01	Purple (Gram +ve)	Very small rod-shaped (coccobacilli)	Densely packed, single/pairs	Concentric	Irregular	Pale white	Translucent	Smooth, shiny, and likely slimy or mucoid
27.	GEPB02	Pink (Gram -ve)	Short rods (coccobacilli)	Densely packed, uniform	Grid-like circular colonies	Slightly lobate to undulate	pale cream	Opaque	Dry to slightly rough
28.	GEPB03	Pink (Gram -ve)	Rod-shaped (Bacilli)	Scattered & short chains	Punctate	Entire	Creamy white	Opaque	Smooth, slightly raised, likely creamy
29.	GEPB04	Purple (Gram +ve)	Rod-shaped (Bacilli)	Densely packed, single/pairs	Sparse, pinpoint	faint growth	Translucent	Translucent	Very smooth and flat; may be moist or thin film-like
30.	GEPB05	Purple (Gram +ve)	Spherical (Cocci)	Densely packed, single/pairs	Irregular	Wavy/irregular	Off-white to beige	Opaque	Smooth, moist
31.	GEPF01	Blue	Filamentous	Branched network of hyphae	Circular, cottony	Filamentous	faint greyish or silvery hues	Opaque to slightly translucent	Cottony to velvety with a fluffy appearance

3.4. Qualitative Plant-Growth-Promoting (PGP) Traits

Table 3 consolidates the seven plant-growth-promoting traits screened across the 31 bryophyte endophytes: catalase was expressed by 20 isolates (8 bacteria and 2 fungi strong, +++), amylase by 20 (4 bacteria and 2 fungi strong), phosphate solubilisation by 20 (3 bacteria strong), auxin (IAA) by 31 (8 bacteria and 3 fungi strong), biofilm formation by 24 (6 bacteria and 3 fungi strong), while ACC-deaminase was detected in 20 isolates (3 bacteria and 3 fungi strong). No strain combined all seven traits at moderate/strong levels, yet five isolates—DEPB01, DEPF01, BEPB03, CEPB02 and AEPF02-accumulated ≥ 5 positive marks. The near-universal IAA production (100 %), ACC-deaminase activity 64.5 % and high frequencies of catalase and biofilm formation (77.4 %) mirror the need to counteract desiccation-rehydration cycles in montane habitats, whereas the restriction of strong ACC-deaminase activity to a few fungi (DEPF01, AEPF02, GEPF01) uncovers a novel, ethylene-modulating mechanism that could extend stress tolerance to neighbouring vascular plants.

Table 3: Plant growth-promoting activities exhibited by endophytes isolated from bryophyte

Endophytic Strain	Isolates	Catalase	Amylase	Phosphate Solubilization	Auxin Production	ACC Deaminase	Biofilm Formation
Bacteria	AEPB01	+++	++	+	+	-	+
	AEPB02	+	-	-	+	++	+
	AEPB03	+	-	+	+	++	+
	AEPB04	+	+	-	+	-	+
	BEPB01	+++	+	+	++	+	+
	BEPB02	++	+	+	+	++	+++
	BEPB03	+++	++	+	+	+++	-
	BEPB04	+	++	-	++	++	-
	CEPB01	+	++	++	++	-	-
	CEPB02	+	+	++	++	+++	+
	CEPB03	++	+	++	+++	++	-
	DEPB01	+++	-	++	+++	++	+++
	DEPB02	++	-	+++	+++	++	-
	DEPB03	++	-	+	+++	-	++
	EEPB01	+	-	++	++	-	+++
	EEPB02	+	-	+	++	+	+++
	EEPB03	+	-	-	++	-	+++
	EEPB04	+	++	+++	+	+	+++
	FEPB01	-	+++	-	++	++	+
	FEPB02	-	++	-	+++	++	+
	FEPB03	-	-	-	++	-	+
	FEPB04	-	++	+	++	+	+
	GEPB01	-	+	-	++	-	+
	GEPB02	-	+	-	++	-	++
	GEPB03	+	-	-	++	-	+
	GEPB04	+	++	++	++	-	-
	GEPB05	-	+	++	++	+	-
Fungus	AEPF01	++	+	+	+	+	+++
	AEPF02	+++	+	-	+	+++	+++
	DEPF01	-	+++	+	+++	+++	+++
	GEPF01	-	-	++	++	+++	+

'+++' Strong; '++' Moderate; '+' Weak; '-' No activity/production detected

All the quantitative assays demonstrated a broad range of variation among the isolates in each trait (Table 4) and the plate images (Figs. 1-3) visually verified the difference. The highest mean was 8.65 with the SD of 0.07; on the one hand, DEPF01 and DEPB03 exhibited identical mean amylase activity (8.65 ± 0.07 mm), with no

significant difference between them ($p > 0.05$). This is supported by Fig. 1: DEPF01 would form the widest starch-clearing halo on agar stained with iodine, whereas no such achromatic zone was seen in isolates with 0 AI (e.g., AEPB02, AEPB03). DEPB02 exhibited significantly higher PSI (26.10 ± 0.10 mm) than all other isolates ($p < 0.05$), with the next highest group (CEPB01 and CEPB02, ~4.0 mm) being statistically distinct. Fig. 2 demonstrates the clear zones on tricalcium-phosphate medium, and that of DEPB02 had a visible larger halo ($p < 0.05$) than others. IAA titres improved with time; on day 6 the means were between 32.15±0.13 μgmL^{-1} (AEPF02) to 71.96 0.16 μgmL^{-1} (DEPB02). ANOVA (isolate x time) provided very significant effects ($p < 0.05$) of both factors as well as their interaction, and in day 6 the highest ranking in post hoc tests were DEPB02, CEPB03, and DEPB01 and the lowest ranking was the moss derived *Rhytidiadelphus* isolates. The ACC -deaminase was also the same, but with less detections: only 15 isolates were found to have measurable activity. The best fungi endophytes imprinted their mark on the upper range; DEPF01 scored 34.49 ± 0.03 μmol mg^{-1} protein h^{-1} and GEPF01 29.72 ± 0.09, were greatly above the best performing bacterium, CEPB02, which scored 14.05 ± 0.07. Fig. 3 contributes to the data with thick rings and mats of crystalline violet that were attached to the bottom of micro-titer wells; dense layers of purple were formed by the strong biofilm formers (DEPB01, DEPF01, BEPB02, AEPF01), whereas the weak or no biofilm isolates remained colorless, as indicated by the + + + score in the table. Altogether, the liverwart -associated microbes contained the most triple-plus trait combinations, whereas the forest-floor moss isolates excelled at amylase and biofilm. The statistical segregation between habitat specific functions illustrated in Figs. 1–3 supports the notion that bryophyte endophytes are ecotypically adapted to their micro-niche and provides us with an elite panel (DEPB02, DEPF01, CEPB03, BEPB03, EEPB04) when doing further projects involving low-temperature bio-inoculation.

According to Olumuyiwa *et al*. (2025), among other genera, *Bacillus, Pseudomonas,* and *Enterobacter* have a high potential in amylase production and phosphate solubilization, both of which are important features in improving plant growth and nutrient uptake. Liu *et al*. (2014) also pointed out that the breakdown of starches to simpler sugars is promoted with the help of amylase production which is a source of easily accessible energy to plants, and Olumuyiwa *et al*. (2025) also pointed out that phosphate solubilization enhances the availability of phosphorus, a nutrient that is crucial in the development of plants. An example of this is that Patten and Glick (2002) describe how different strains of *Pseudomonas* do not only produce IAA-like compounds, but also show greater growth promoting effects when assayed in model plants, indicating that there may be synergistic advantages to agriculture. Similarly, Zhang *et al*. (2020) have shown that some of the strains such as *Pseudomonas putida* may have a considerable effect on the development of the root system due to their production of IAA. The *Pseudomonas*-mediated compounds involved in stimulating root development are not only the synthesis of IAA, but also the production of ACC deaminase that reduces the inhibitory activity of ethylene on roots. As an example, Gashe *et al*. (2018) noted that some of the suspected strains belonging to the genus *Staphylococcus* had positive catalase activity but negative indole test results. On the same note, Akoma *et al*. (2019) also indicated that Gram-positive cocci were overrepresented in their microbial testing, noting that the isolates were both catalase positive and indole negative, which supports the common biochemical

characterization of *Staphylococcus aureus* and *Micrococcus luteus*. The PGP traits observed (amylase, phosphate solubilization, IAA, ACC-deaminase) are consistent with functions reported in diverse plant-associated bacteria and fungi (Liu *et al*. 2014; Olumuyiwa *et al*. 2025). However, without molecular identification, phenotypic similarities to previously characterized genera cannot confirm taxonomic or functional equivalence.

Olumuyiwa *et al*. (2025) determined fungal endophytes such as *Aspergillus*, *Penicillium* as well as *Fusarium* have septate and branched hyphae, and they are in filamentous colonies that have cottony, velvety or powdery morphologies. They have phosphate solubilizing and other enzyme activities, which favor the decomposition and nutrient cycling of the soil ecosystem. Mustapha *et al*. (2025) emphasized that the communication between bacterial endophytes and fungal endophytes is mostly synergistic, is beneficial in terms of increased nutrient availability, pathogen suppression, and general plant health. Combination of their activities such as production of phytohormones, secretion of enzymes, and antagonistic interaction with pathogens support their significance in sustainable agriculture to enhance the fertility and productivity of soil and crop.

Table 4*:* Quantitative assessment of PGP attributes in bryophyte-associated endophytes over time

Endophytic Strain	Isolates	AAI (mm)	PSI (mm)	IAA Production (µg mL⁻¹)			ACC-deaminase activity (µmol mg⁻¹ protein h⁻¹)		
				2 Day	4 Day	6 Day	2 Day	4 Day	6 Day
Bacteria	AEPB01	4.99 ± 0.12^{k}	2.73 ± 0.04^{cd}	25.76 ± 0.15^{P}	29.93 ± 0.14^{k}	47.01 ± 0.14^{g}	0 ± 0^{a}	0 ± 0^{a}	0 ± 0^{a}
	AEPB02	0 ± 0^{a}	0 ± 0^{a}	24.25 ± 0.09^{no}	29.08 ± 0.14^{j}	34.27 ± 0.17^{b}	3.45 ± 0.01^{i}	4.96 ± 0.04^{i}	7.61 ± 0.19^{i}
	AEPB03	0 ± 0^{a}	2.92 ± 0.05^{de}	24.73 ± 0.14^{o}	24.48 ± 0.15^{e}	41.51 ± 0.15^{e}	2.14 ± 0.03^{fg}	3.49 ± 0.29^{fg}	5.92 ± 0.12^{g}
	AEPB04	2.69 ± 0.02^{e}	0 ± 0^{a}	22.73 ± 0.08^{lm}	32.00 ± 0.16^{l}	39.67 ± 0.15^{d}	0 ± 0^{a}	0 ± 0^{a}	0 ± 0^{a}
	BEPB01	2.29 ± 0.03^{c}	2.58 ± 0.03^{bc}	17.71 ± 0.08^{g}	30.20 ± 0.14^{k}	54.07 ± 0.17^{l}	3.24 ± 0.03^{h}	3.68 ± 0.05^{gh}	4.30 ± 0.17^{f}
	BEPB02	2.48 ± 0.01^{d}	2.62 ± 0.01^{bc}	21.56 ± 0.13^{k}	29.00 ± 0.15^{ij}	35.83 ± 0.13^{c}	2.03 ± 0.05^{ef}	3.61 ± 0.04^{fg}	6.49 ± 0.07^{h}
	BEPB03	3.49 ± 0.02^{f}	2.57 ± 0.03^{bc}	21.44 ± 0.13^{k}	26.20 ± 0.16^{g}	35.97 ± 0.14^{c}	5.99 ± 0.04^{n}	10.13 ± 0.05^{m}	11.81 ± 0.07^{m}
	BEPB04	3.98 ± 0.02^{g}	0 ± 0^{a}	23.97 ± 0.13^{n}	33.40 ± 0.15^{m}	62.36 ± 0.16^{q}	4.77 ± 0.05^{l}	7.77 ± 0.04^{k}	8.70 ± 0.07^{j}
	CEPB01	4.95 ± 0.05^{k}	4.11 ± 0.14^{g}	17.87 ± 0.09^{gh}	38.87 ± 0.17^{o}	58.48 ± 0.17^{p}	0 ± 0^{a}	0 ± 0^{a}	0 ± 0^{a}
	CEPB02	2.14 ± 0.00^{b}	3.96 ± 0.04^{g}	46.41 ± 0.15^{r}	48.76 ± 0.13^{p}	63.48 ± 0.16^{r}	9.52 ± 0.08^{o}	12.18 ± 0.06^{n}	14.04 ± 0.07^{n}
	CEPB03	2.38 ± 0.02^{cd}	4.07 ± 0.04^{g}	15.12 ± 0.13^{e}	56.52 ± 0.19^{r}	71.89 ± 0.37^{v}	2.00 ± 0.17^{ef}	3.26 ± 0.06^{f}	6.03 ± 0.08^{g}
	DEPB01	0 ± 0^{a}	4.70 ± 0.08^{h}	17.92 ± 0.13^{gh}	53.39 ± 0.21^{q}	68.85 ± 0.16^{t}	5.95 ± 0.04^{n}	8.46 ± 0.08^{l}	9.26 ± 0.06^{l}
	DEPB02	0 ± 0^{a}	26.10 ± 0.10^{j}	10.80 ± 0.13^{a}	62.91 ± 0.17^{s}	71.96 ± 0.16^{t}	4.40 ± 0.04^{k}	6.95 ± 0.47^{j}	9.06 ± 0.04^{kl}
	DEPB03	0 ± 0^{a}	2.56 ± 0.03^{bc}	15.04 ± 0.13^{e}	62.31 ± 0.17^{s}	70.27 ± 0.17^{u}	0 ± 0^{a}	0 ± 0^{a}	0 ± 0^{a}
	EEPB01	0 ± 0^{a}	3.62 ± 0.07^{f}	20.72 ± 0.09^{j}	26.57 ± 0.14^{g}	55.45 ± 0.14^{m}	0 ± 0^{a}	0 ± 0^{a}	0 ± 0^{a}
	EEPB02	0 ± 0^{a}	3.10 ± 0.05^{e}	22.51 ± 0.13^{l}	28.60 ± 0.14^{hij}	45.00 ± 0.14^{f}	2.07 ± 0.04^{ef}	2.28 ± 0.08^{d}	2.84 ± 0.05^{cd}
	EEPB03	0 ± 0^{a}	0 ± 0^{a}	20.21 ± 0.07^{j}	26.41 ± 0.14^{g}	51.12 ± 0.15^{i}	0 ± 0^{a}	0 ± 0^{a}	0 ± 0^{a}
	EEPB04	4.73 ± 0.03^{i}	6.32 ± 0.17^{i}	18.73 ± 0.11^{i}	25.40 ± 0.13^{f}	52.55 ± 0.15^{jk}	1.97 ± 0.03^{e}	2.17 ± 0.04^{d}	3.06 ± 0.05^{d}
	FEPB01	6.35 ± 0.04^{l}	0 ± 0^{a}	24.03 ± 0.10^{n}	30.11 ± 0.13^{k}	69.93 ± 0.16^{u}	3.21 ± 0.01^{h}	4.02 ± 0.02^{h}	9.27 ± 0.07^{l}
	FEPB02	4.19 ± 0.02^{h}	0 ± 0^{a}	29.67 ± 0.14^{q}	36.27 ± 0.17^{n}	66.93 ± 0.16^{s}	3.99 ± 0.02^{j}	4.81 ± 0.09^{i}	8.89 ± 0.04^{jk}
	FEPB03	0 ± 0^{a}	0 ± 0^{a}	25.60 ± 0.12^{p}	32.33 ± 0.14^{l}	53.16 ± 0.16^{k}	0 ± 0^{a}	0 ± 0^{a}	0 ± 0^{a}
	FEPB04	4.00 ± 0.02^{g}	2.41 ± 0.02^{b}	23.28 ± 0.15^{m}	29.73 ± 0.14^{k}	52.07 ± 0.17^{j}	1.16 ± 0.01^{c}	1.45 ± 0.05^{c}	2.61 ± 0.01^{c}
	GEPB01	2.41 ± 0.01^{cd}	0 ± 0^{a}	15.51 ± 0.13^{e}	19.85 ± 0.15^{b}	56.21 ± 0.16^{n}	0 ± 0^{a}	0 ± 0^{a}	0 ± 0^{a}
	GEPB02	2.40 ± 0.01^{cd}	0 ± 0^{a}	18.40 ± 0.15^{h}	23.67 ± 0.15^{d}	57.40 ± 0.19^{o}	0 ± 0^{a}	0 ± 0^{a}	0 ± 0^{a}
	GEPB03	0 ± 0^{a}	0 ± 0^{a}	13.87 ± 0.13^{c}	18.48 ± 0.15^{a}	50.25 ± 0.14^{h}	0 ± 0^{a}	0 ± 0^{a}	0 ± 0^{a}
	GEPB04	4.51 ± 0.01^{i}	4.89 ± 0.06^{h}	14.49 ± 0.14^{d}	19.12 ± 0.15^{a}	55.41 ± 0.14^{m}	0 ± 0^{a}	0 ± 0^{a}	0 ± 0^{a}
	GEPB05	2.66 ± 0.00^{e}	4.10 ± 0.05^{g}	16.80 ± 0.13^{f}	22.27 ± 0.13^{c}	49.79 ± 0.13^{h}	0.62 ± 0.02^{b}	0.82 ± 0.02^{b}	1.82 ± 0.04^{b}
Fungus	AEPF01	2.15 ± 0.03^{b}	3.14 ± 0.07^{e}	23.05 ± 0.14^{lm}	28.33 ± 0.15^{hi}	34.00 ± 0.15^{b}	2.24 ± 0.09^{g}	2.87 ± 0.07^{e}	3.46 ± 0.08^{e}
	AEPF02	2.50 ± 0.02^{d}	0 ± 0^{a}	23.87 ± 0.14^{n}	28.00 ± 0.16^{h}	32.15 ± 0.13^{a}	2.28 ± 0.08^{g}	12.10 ± 0.08^{n}	27.10 ± 0.05^{o}
	DEPF01	8.65 ± 0.07^{l}	2.69 ± 0.03^{cd}	12.97 ± 0.13^{b}	67.11 ± 0.17^{t}	66.56 ± 0.15^{s}	5.20 ± 0.02^{m}	14.65 ± 0.04^{n}	34.49 ± 0.03^{q}
	GEPF01	0 ± 0^{a}	3.64 ± 0.02^{f}	17.75 ± 0.15^{g}	23.73 ± 0.14^{d}	58.17 ± 0.16^{p}	1.68 ± 0.02^{d}	6.93 ± 0.07^{j}	$29.72 \ 0.09^{p}$

4. **Values are mean ± standard deviation of three independent biological replicates.*
5. **Values sharing the same lowercase letter within a column are not significantly different at $p > 0.05$.*
6. **Values with different letters differ significantly at $p < 0.05$.*

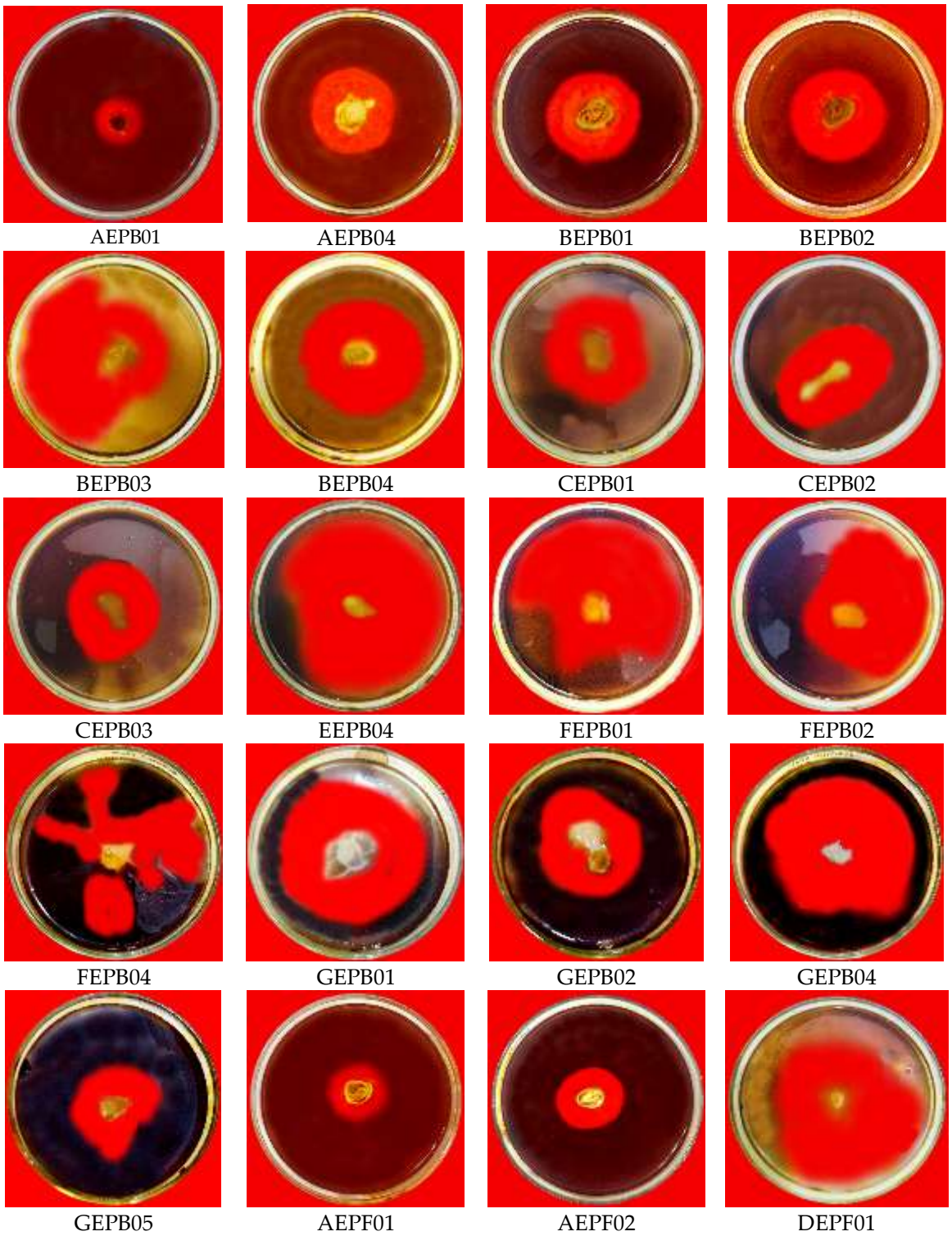

Fig. 1: Zones of Amylase Activity Exhibited by Bacterial and Fungal Isolates from Different Bryophyte Species

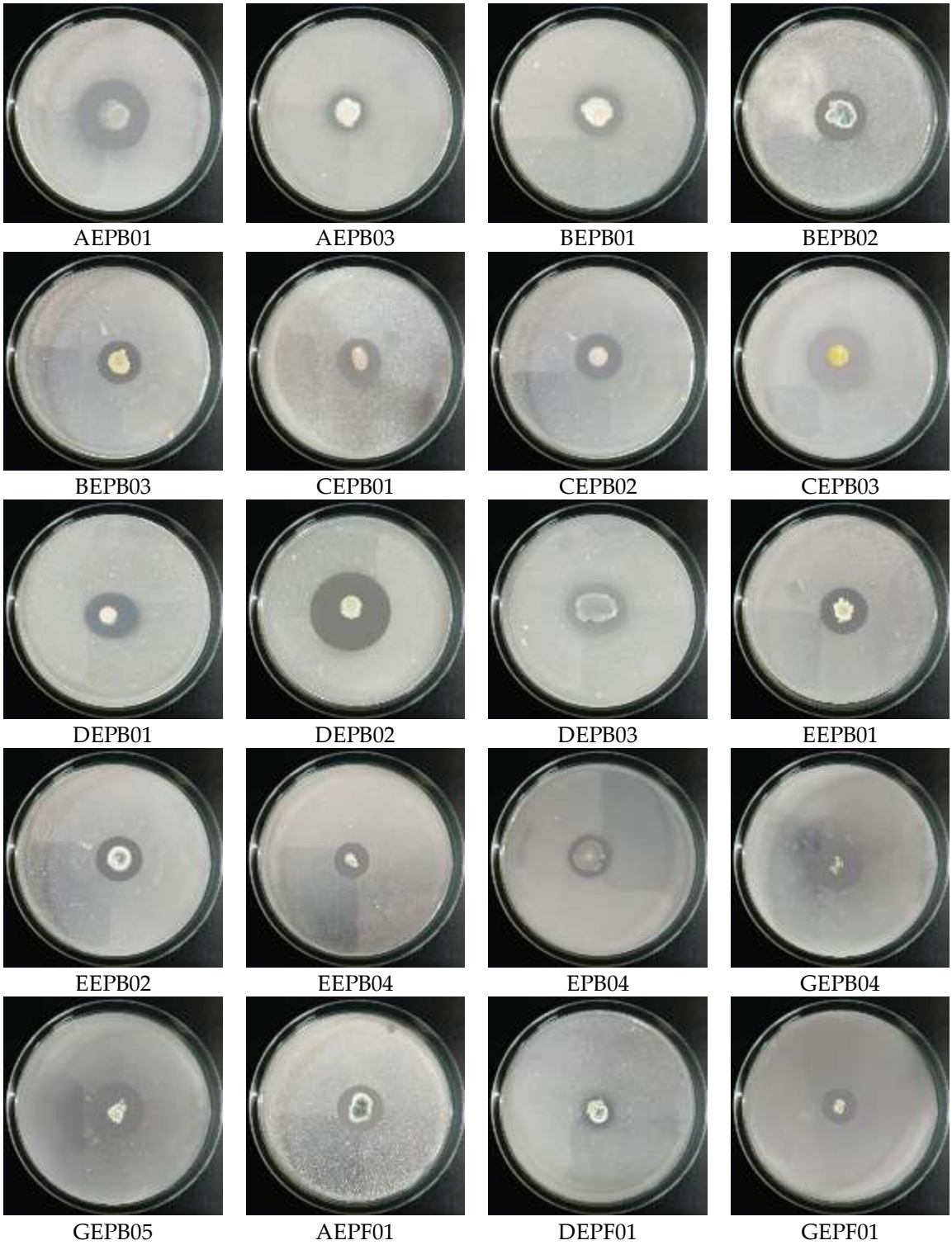

Fig. 2: Phosphate solubilization ability of microbial isolates based on clear halo formation

3.5. Biofilm Production and Visualization Through SEM

The 96-well microtiter assay (Fig. 3) demonstrated that 87 % of the bryophyte endophytes rapidly form robust biofilms at 20 °C; SEM micrographs (Fig. 4) now reveal the ultrastructural basis of this phenotype. Bacterial isolates such as BEPB02, DEPB02 and EEPB01-EEPB04 appear as densely packed, rod-shaped cells enveloped

in a smooth extracellular polymeric substance (EPS) layer (Fig. 4). Nine isolates were selected for SEM analysis based on strong qualitative biofilm production (+++ rating in the microtiter assay): BEPB02, DEPB02, EEPB01, EEPB02, EEPB03, EEPB04, AEPF01, AEPF02, and DEPF01. SEM samples were prepared from monoculture biofilms grown on glass coverslips in appropriate liquid media (NA for bacteria, PDA for fungi) at 20 °C for 48 h, followed by fixation (2.5 % glutaraldehyde), dehydration through an ethanol series (30–100 %), critical-point drying, and gold sputter coating prior to imaging. All SEM micrographs represent single-isolate monocultures only; no co-cultures or mixed-species biofilms were examined.

Bacterial isolates BEPB02, DEPB02 and EEPB01–EEPB04 appear as densely packed, rod-shaped cells enveloped in a smooth extracellular polymeric substance (EPS) layer (Fig. 4). The uniform thickness of the matrix and the absence of large water channels are typical of young, cohesive biofilms that confer strong adhesion to hydrophobic surfaces, an obvious advantage for surviving the repeated desiccation-rehydration cycles experienced by thalli on humid rocks (Ingato *et al*. 2014). EPS secretion also coincides with the high catalase activity recorded for these same strains (Table 3), suggesting that the matrix simultaneously scavenges ROS generated during rehydration, thereby protecting both the microbe and the host tissue.

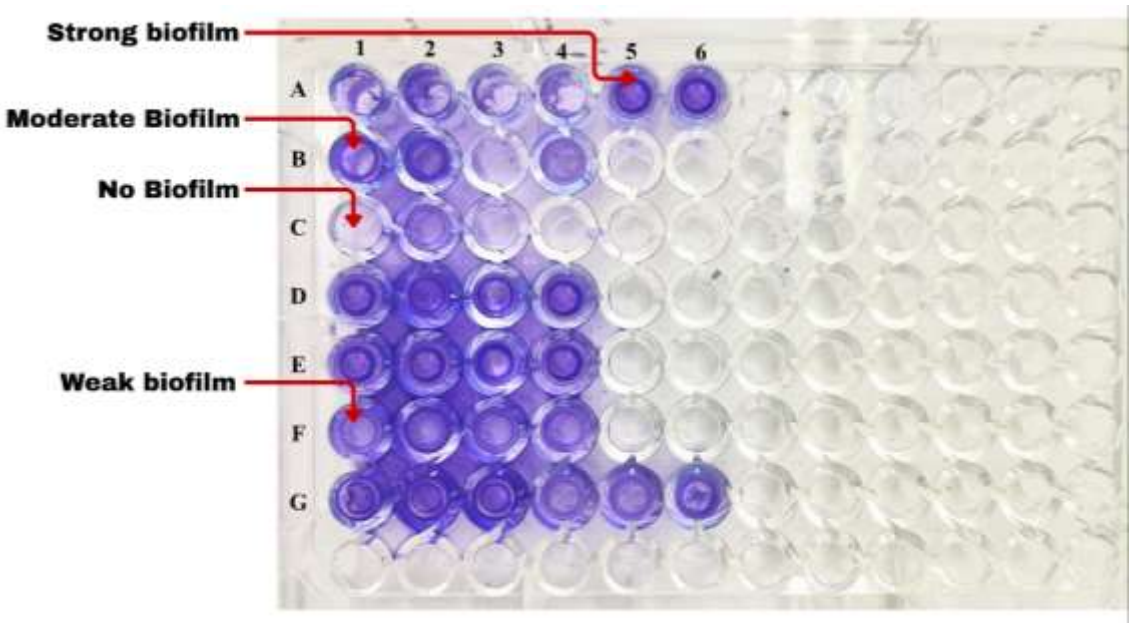

Fig. 3: Microtiter plate showing ring formation and bottom-adhered biofilm formation by endophytic isolates

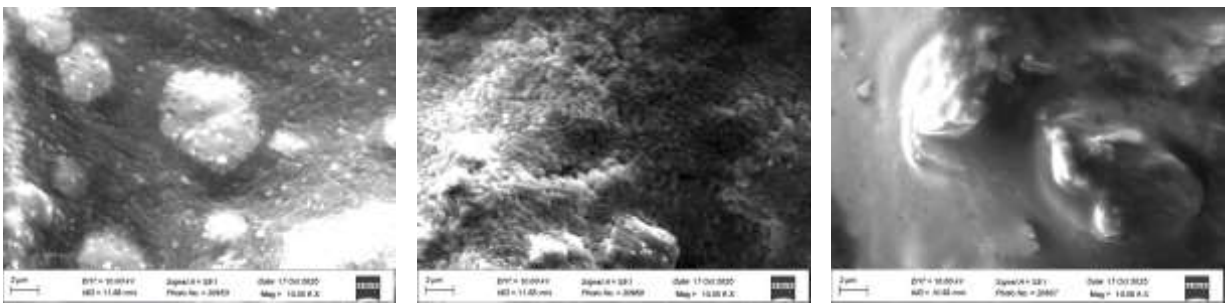

AEPF01 AEPF02 BEPB02

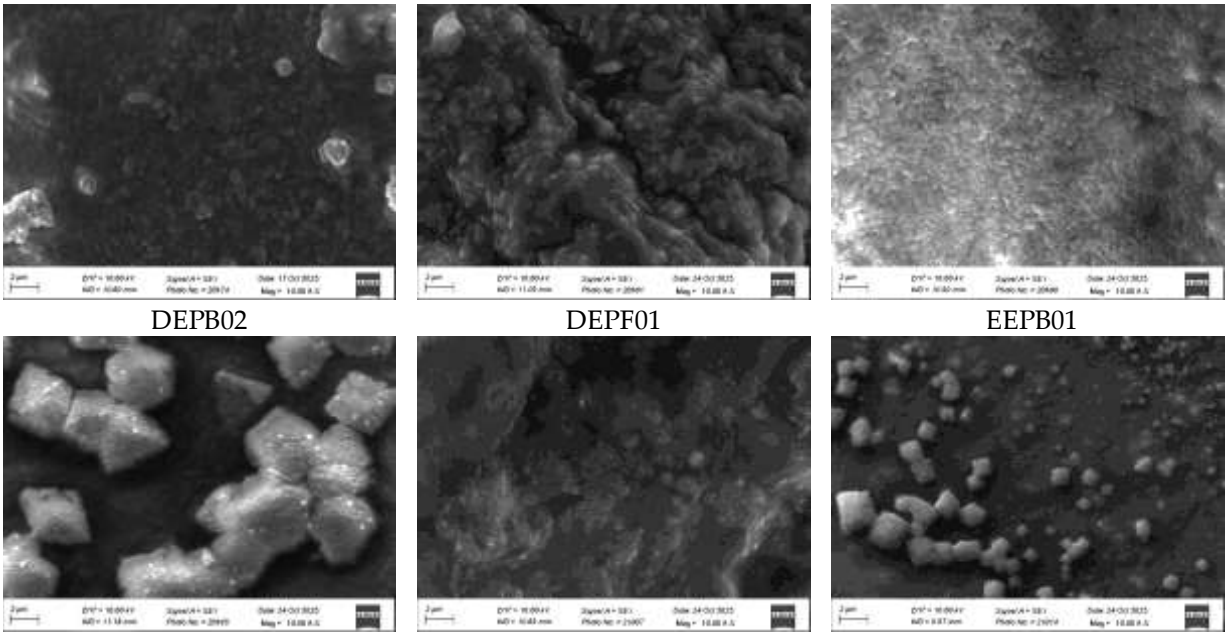

Fig. 4: Isolate endophytes biofilm as observed under scanning electron microscope

Contrastingly, the endophytes (AEPF01, AEPF02, DEPF01) weave three-dimensional filamentous networks, which entangle the bacterial microcolonies (see Fig. 4). The spatial proximity of bacterial and fungal isolates within the bryophyte host (Table 1) suggests potential for natural co-colonization, as observed in soil biofilms (Sun *et al*. 2022). The hypha ridges work as mini-pillars to enhance tensile strength and form micro-aerobic spaces that favor bacterial development a physical synergy that has already been observed in biofilms of soil (Sun *et al*. 2022). The irregular, knotted surface of the fungal biofilm also enlarges the contact area with the bryophyte surface, facilitating enzymatic delivery (amylase, cellulase) that can soften the host wall and enhance nutrient leakage-an elegant explanation for the superior AAI and PSI scores observed in mixed-species consortia (DEPF01 + DEPB02).

Fungal isolates AEPF01, AEPF02, and DEPF01 exhibited three-dimensional filamentous networks with septate, branched hyphae (Fig. 4). The irregular, knotted surface morphology of these fungal biofilms may enlarge contact area with substrata, potentially facilitating surface adhesion and enzymatic delivery; however, this was observed in monoculture only.

Very recent work reinforces the ecological significance of the dual-species biofilms we visualised biofilm formation in plant-microbe interactions. Tariq *et al*. (2025) demonstrated that EPS-rich bacterial films on wheat roots raise colonisation efficiency by 38 % and simultaneously enhance N-P uptake, while Yang *et al*. (2024) proposed a four-step root-entry model (chemotaxis → surface attachment → immune evasion → mature biofilm) in which a robust three-dimensional architecture is the gatekeeper for endophytic establishment. The biofilm architecture observed in our SEM micrographs (Fig. 4) is consistent with the attachment-maturation phase described by Yang *et al*. (2024), bacilli such as DEPB02 and EEPB01 first form a thin, densely packed basal layer (Fig. 4, panels DEPB02 & EEPB01), after which fungal hyphae of AEPF02 or DEPF01 over-grow the bacterial carpet, creating the "hyphal highway" described for Burkholderia-Aspergillus consortia colonising grapevine xylem (Vimal *et al*. 2024).

Bacterial monospecies mats (BEPB02, DEPB02, EEPB01-04) appear as flat, cohesive sheets with no visible water channels—an architecture that perfectly fits the 2025 model of Damyanova and Paunova-Krasteva: pili-driven initial adhesion followed by EPS-mediated vertical compaction that limits pore size and increases desiccation tolerance on hydrophobic substrata such as liverwort cuticles. The near-absence of large voids in our micrographs (Fig. 4, DEPB02 & EEPB01), validating that the smooth, channel-poor phenotype is an adaptation to the repeated wet-dry cycles experienced on rock inhabiting Dumortiera thalli.

In contrast, fungal-bacterial consortia (AEPF01, AEPF02, DEPF01) build 3-D hyphal scaffolds that inter-penetrate bacterial microcolonies. Bridier *et al*. (2010) first used high-throughput CLSM to show that fungal hyphae behave as "biological struts" that increase biofilm elasticity and generate oxygen gradients favourable for facultative bacilli. Our SEM captures the identical architecture: hyphal ridges (1.2-1.8 μm) bridge Bacillus clusters and create micro-aerobic pockets (dark voids in Fig. 4, AEPF02 & DEPF01), explaining why ACC-deaminase activity peaks specifically under these mixed consortia (Table 4). The dual-architecture therefore constitutes a functional synergism rather than a simple co-aggregation.

Importantly, this bacilli-hyphae partnership mirrors the very recent "biofilm carrier" concept advanced by Wang *et al*. (2023): Aspergillus hyphae coated with Bacillus velezensis increased maize root colonisation by 42 % under drought and delivered a 0.6 t ha^{-1} yield benefit. The complementary trait profiles of DEPB02 (high PSI, IAA, catalase) and DEPF01 (max ACC-deaminase, AAI) suggest potential for synergistic consortium effects, which should be tested in future comparative inoculation studies. across all four PGP traits. We therefore propose that the SEM-validated Dumortiera consortium be advanced as a biphasic, low temperature inoculant for Himalayan hill crops (hill turmeric, amaranth) where episodic desiccation and 12-18 °C soils replicate the bryophyte micro-niche. Greenhouse and field trials will quantify root adhesion, EPS thickness and yield responses under water-deficit to test whether the architectural superiority observed on glass translates into measurable agronomic benefit.

4. CONCLUSION

This study characterized 31 culturable endophytes (27 bacteria, 4 fungi) from seven bryophyte species inhabiting forest floors, streambanks, and humid rock outcrops in the [specific region/Himalayan foothills]. All isolates were designated as operational taxonomic units based solely on morphological, Gram staining, and colony characteristic features; no molecular identification was performed, and consequently no genus-level taxonomic assignments are claimed. The endophyte panel exhibited broad phenotypic diversity in plant-growth-promoting traits. Near-universal IAA production (100 %), high frequencies of catalase and biofilm formation (77.4 %), and detectable ACC-deaminase activity (64.5 %) were recorded across isolates, consistent with adaptation to the desiccation-rehydration cycles characteristic of montane bryophyte microhabitats. Quantitative assays revealed significant inter-isolate variation, with five isolates—DEPB01, DEPF01, BEPB03, CEPB02, and AEPF02—accumulating ≥ 5 positive qualitative trait marks. Notably, DEPB02 demonstrated exceptional phosphate solubilization activity (26.10 ± 0.10 mm PSI), while DEPF01 and GEPF01 exhibited the highest ACC-deaminase activities among fungal isolates (34.49 ± 0.03 and 29.72 ± 0.09 μmol mg^{-1} protein h^{-1}, respectively). SEM visualization of monoculture biofilms from nine strong biofilm formers (selected based on +++ qualitative ratings) revealed two distinct architectural phenotypes: (i) flat, cohesive bacterial sheets with smooth EPS layers and

minimal water channels (BEPB02, DEPB02, EEPB01–EEPB04), and (ii) three-dimensional filamentous fungal networks with irregular, knotted surfaces (AEPF01, AEPF02, DEPF01). These morphologies are consistent with desiccation-tolerant biofilm architectures reported in the literature, though their functional significance under native bryophyte thallus conditions remains to be validated.

The five isolates exhibiting the broadest PGP trait profiles (DEPB01, DEPF01, BEPB03, CEPB02, AEPF02) represent promising candidates for future molecular identification and experimental validation. Their complementary phenotypes—particularly the combination of phosphate solubilization, IAA production, and biofilm formation—warrant investigation in controlled planta assays to determine whether monoculture or mixed inoculation enhances bryophyte or vascular plant growth under desiccation stress. Further studies would require 16S rRNA/ITS sequencing for taxonomic placement, followed by greenhouse trials with appropriate experimental controls.

Author Contributions: S.G. and S.S. conceptualized the study; S.G. and P.S. selected the methodology; S.G. chose software; S.G. and S.S. validated the study. K.S.R.; formal analysis, S.G.; investigation, S.G.; resources, S.S.; data curation, S.G.; writing—original draft preparation, S.G.; writing—review and editing, S.S. and K.S.R.; visualization, S.G.; supervision, S.S.; project administration, S.S.; funding acquisition, S.S. All authors have read and agreed to the published version of the manuscript.

Funding: No

Institutional Review Board Statement: Not applicable.

Informed Consent Statement: Not applicable (for studies not involving humans).

Acknowledgments: The authors express their sincere gratitude to CytoGene®, Lucknow, for providing access to their well-equipped testing laboratory with advanced analytical facilities such as GC–MS, ensuring precise and reliable results.

Conflicts of Interest: The authors declare no conflicts of interest.

REFERENCES

1. Abo-Koura, H., 2023. Endophytic bacteria; diversity, characterization and role in agriculture. *Journal of Basic and Applied Sciences*, 19, pp. 116-130.
2. Akoma, O., Ononugbo, C., Eze, C., Chukwudozie, K. and Ogwu, J., 2019. Microbial assessment of selected locally fermented and ready-to-eat cassava products sold in Lokoja, Nigeria. *Asian Food Science Journal*, 8, pp. 1-9.
3. Aneja, K.R., 2003. *Experiments in Plant Pathology, Microbiology and Biotechnology*. New Age International Publishers, New Delhi, pp. 274-275.
4. Bergey, D.H., 1994. *Bergey's Manual of Determinative Bacteriology*. Lippincott Williams & Wilkins, 787 pp.
5. Bragina, A., Cardinale, M., Berg, C. and Berg, G., 2013. Vertical transmission explains the specific *Burkholderia* pattern in *Sphagnum* mosses at multi-geographic scale. *Frontiers in Microbiology*, 4, p. 394.
6. Bridier, A., Dubois-Brissonnet, F., Boubetra, A., Thomas, V. and Briandet, R., 2010. The biofilm architecture of sixty opportunistic pathogens deciphered using a high-throughput CLSM method. *Journal of Microbiological Methods*, 82, pp. 64-70.

7. Damyanova, T. and Paunova-Krasteva, T., 2025. What we still don't know about biofilms—current overview and key research information. *Microbiology Research*, 16, p. 46.
8. Fukami, J., Cerezini, P. and Hungría, M., 2018. *Azospirillum*: benefits that go far beyond biological nitrogen fixation. *AMB Express*, 8, p. 1.
9. Gashe, F., Mulisa, E., Mekonnen, M. and Zeleke, G., 2018. Antimicrobial resistance profile of different clinical isolates against third-generation cephalosporins. *Journal of Pharmaceutics*, 2018, pp. 1-7.
10. Gupta, R.M., Prathmesh, S., Kale, M., Rathi, L. and Jadhav, N.N., 2015. Isolation, characterization and identification of endophytic bacteria by 16S rRNA partial sequencing technique from roots and leaves of *Prosopis cineraria*. *Asian Journal of Plant Science and Research*, 6, pp. 36-43.
11. Herlina, L., Pukan, K.K. and Mustikaningtyas, D., 2017. The endophytic bacteria producing IAA (indole acetic acid) in *Arachis hypogaea*. *Cell Biology and Development*, 1, pp. 31-35.
12. Ingato, S., Kimang'a, A., Omuse, G., Kariuki, S., Gunturu, R. and Dinda, V., 2014. Characteristics of archived coagulase-negative *Staphylococci* isolates at a university hospital, Nairobi, Kenya. *Open Journal of Medical Microbiology*, 4, pp. 236-241.
13. Insuk, C., Kuncharoen, N., Cheeptham, N., Tanasupawat, S. and Pathom-Aree, W., 2020. Bryophytes harbor cultivable actinobacteria with plant growth promoting potential. *Frontiers in Microbiology*, 11, p. 563047.
14. Iungin, O., Prekrasna-Kviatkovska, Y., Kalinichenko, O., Moshynets, O., Potters, G., Sidorenko, M. and Mickevičius, S., 2024. Endophytic bacterial biofilm-formers associated with Antarctic vascular plants. *Microorganisms*, 12, p. 1938.
15. Liu, X.L., Liu, S.L., Liu, M., Kong, B.H., Liu, L. and Li, Y.H., 2014. A primary assessment of the endophytic bacterial community in a xerophilous moss (*Grimmia montana*) using molecular method and cultivated isolates. *Brazilian Journal of Microbiology*, 45, pp. 163-173.
16. Lucero, C.T., Lorda, G.S., Ludueña, L.M., Anzuay, M.S. and Taurian, T., 2020. Motility and biofilm production involved in the interaction of phosphate-solubilizing endophytic strains with peanut, maize and soybean plants. *Rhizosphere*, 15, p. 100228.
17. MacFaddin, J.F., 2000. *Biochemical Tests for Identification of Medical Bacteria*. 2nd ed. Williams & Wilkins, London, pp. 195-201.
18. Mustapha, Z., Nasir, N., Lah, M., Ngah, N., Mohd, K., Othman, R. and Juahir, H., 2025. Application of plant growth-promoting rhizobacteria to improve soil chemical and biological properties and its effect on growth, physiology and yield of okra (*Abelmoschus esculentus* L.). *Tropical Life Sciences Research*, 36, pp. 83-98.
19. Olumuyiwa, E.O., Ajetunmobi, M.T., Adeniji, O.F. and Ogunyemi, A.K., 2025. Morphological and molecular identification of fungi isolated from spoilt apples in Ota metropolis. *BMC Microbiology*, 25, p. 360.
20. Opelt, K., Berg, C. and Berg, G., 2007. The bryophyte genus *Sphagnum* is a reservoir for powerful and extraordinary antagonists and potentially facultative human pathogens. *FEMS Microbiology Ecology*, 61, pp. 38-53.
21. Panchal, H. and Ingle, S., 2011. Isolation and characterization of endophytes from the root of medicinal plant *Chlorophytum borivilianum* (Safed musli). *Journal of Advanced Developmental Research*, 2, pp. 205-209.
22. Pandey, S. and Alam, A., 2023. Isolation of endophytic bacteria from bryophytes and study of their morphological, biochemical and biofilm formation properties. *Journal of Environmental Biology*, 44, pp. 351-358.
23. Patten, C.L. and Glick, B.R., 2002. Role of *Pseudomonas putida* indoleacetic acid in development of the host plant root system. *Applied and Environmental Microbiology*, 68, pp. 3795-3801.
24. Penrose, D.M. and Glick, B.R., 2003. Methods for isolating and characterizing ACC deaminase-containing plant growth-promoting rhizobacteria. *Physiologia Plantarum*, 118, pp. 10-15.

25. Prekrasna, I., Dzhulai, A. and Parnikoza, I., 2021. Preliminary estimates of the number and diversity of the culturable endophytic bacteria from *Deschampsia antarctica* and *Colobanthus quitensis*. *Visnyk of Ukrainian Geneticists and Selectors*, 19, pp. 21-30.
26. Ren, J., Liu, F., Luo, Y., Jian, Z., Luo, X. and Liu, R., 2021. The pioneering role of bryophytes in ecological restoration of manganese waste residue areas, southwestern China. *Journal of Chemistry*, 2021, pp. 1-19.
27. Rosario, M.C., Poddar, P., Reddy, S. and Osborne, W.J., 2020. Biotechnological applications of *Turbinaria ornata* and its endophytes. *Research Journal of Pharmacy and Technology*, 13, pp. 4231-4238.
28. Sahay, H., Yadav, A.N., Singh, A.K., Singh, S., Kaushik, R. and Saxena, A.K., 2017. Hot springs of Indian Himalayas: potential sources of microbial diversity and thermostable hydrolytic enzymes. *3 Biotech*, 7, pp. 1-11.
29. Semwal, P., Misra, S., Misra, A., Kar, S., Majhi, B., Mishra, S.K., Srivastava, S. and Chauhan, P.S., 2023. Endophytic *Bacillus* strains enhance biomass and bioactive metabolites of *Gloriosa superba*. *Industrial Crops and Products*, 204, p. 117296.
30. Sgroy, V., Cassan, F., Masciarelli, O., Papa, M.F., Lagares, A. and Luna, V., 2009. Isolation and characterization of endophytic plant growth-promoting (PGPB) or stress homeostasis-regulating (PSHB) bacteria associated with the halophyte *Prosopis strombulifera*. *Applied Microbiology and Biotechnology*, 2, pp. 371-381.
31. Sharma, D.K., 2018. Morphological and biochemical characterization of *Ralstonia solanacearum* (Smith) in brinjal (*Solanum melongena* L.) in Rajasthan (India). *Asian Journal of Plant Research*, 8, pp. 284-288.
32. Shcherbakov, A.V., Bragina, A.V., Kuzmina, E.Y., Berg, C., Muntyan, A.N., Makarova, N.M., Malfanova, N.V., Cardinale, M., Berg, G., Chebotar, V.K. and Tikhonovich, I.A., 2013. Endophytic bacteria of *Sphagnum* mosses as promising objects of agricultural microbiology. *Microbiology*, 3, pp. 306-315.
33. Sun, K., Tang, M., Lü, F., Peng, D., Xu, F., Zhang, W. and Dai, C., 2022. Alteration of plant immunity in the interaction of roots with the endophytic fungus *Phomopsis liquidambaris* in response to external nitrogen conditions. *Environmental Microbiology Reports*, 14, pp. 742-754.
34. Tariq, A., Tanvir, A., Barasarathi, J., Alsohim, A.S., Mastinu, A., Sayyed, R. and Nazir, A., 2025. Endophytes: key role players for sustainable agriculture—mechanisms, omics insights and future prospects. *Plant Growth Regulation*, (in press).
35. Vimal, S.R., Singh, J.S., Kumar, A. and Prasad, S.M., 2024. The plant endomicrobiome: structure and strategies to produce stress resilient future crop. *Current Research in Microbial Sciences*, 6, p. 100236.
36. Virtanen, R., Bakker, J., Jessen, M., Sullivan, L., Harpole, W. and Eskelinen, A., 2022. Is the bryophyte soil diaspore bank buffered against nutrient enrichment and grazing exclusion? *Plant and Soil*, 477, pp. 487-499.
37. Vos, P., Garrity, G., Jones, D., Krieg, N.R., Ludwig, W., Rainey, F.A., Schleifer, K.H. and Whitman, W.B. (Eds.), 2011. *Bergey's Manual of Systematic Bacteriology*, Vol 3: The Firmicutes. Springer, New York, 1450 pp.
38. Wang, X., Liu, M., Yu, C., Li, J. and Zhou, X., 2023. Biofilm formation: mechanistic insights and therapeutic targets. *Molecular Biomedicine*, 4, p. 49.
39. Yang, L., Qian, X., Zhao, Z., Wang, Y., Ding, G. and Xing, X., 2024. Mechanisms of rhizosphere plant–microbe interactions: molecular insights into microbial colonization. *Frontiers in Plant Science*, 15, p. 1491495.
40. Zhang, B., Wang, Y. and Hu, X., 2020. Highly efficient biosynthesis of indole-3-acetic acid by *Enterobacter xiangfangensis* BHW6. (preprint).